

Time-interleaved system mismatch estimation based on correlation function and particle swarm optimization algorithm

Cite as: Rev. Sci. Instrum. 93, 104702 (2022); doi: 10.1063/5.0103225

Submitted: 14 June 2022 • Accepted: 1 September 2022 •

Published Online: 4 October 2022



View Online



Export Citation



CrossMark

Yanze Zheng,¹ Naixin Zhou,¹ Yijiu Zhao,^{1,2,a)} and Sicheng Sun¹

AFFILIATIONS

¹ School of Automation Engineering, University of Electronic Science and Technology of China, Chengdu 611731, China

² Shenzhen Institute for Advanced Study, UESTC, Shenzhen 518110, China

^{a)}Author to whom correspondence should be addressed: yijiuzhao@uestc.edu.cn

ABSTRACT

The time-interleaved analog-to-digital converters (TIADCs) technique is an efficient solution to improve the sampling rate of the acquisition system with low-speed ADCs. However, channel mismatches such as gain mismatch, time skew mismatch, and offset mismatch may seriously degrade the performance of TIADC. Furthermore, for high-speed signal acquisition, the gain and time skew mismatches would vary with the signal frequency, and the traditional fixed model does not work any longer. In this paper, a series of sinusoidal signals are adopted to estimate the variable mismatches. First, an autocorrelation-based approach is presented to estimate the gain mismatch. The information about the gain mismatch is extracted from the autocorrelation function of sub-ADC output samples. Then, the time skew mismatch is estimated by utilizing the particle swarm optimization algorithm. The reported simulation results show that the mismatches can be accurately estimated. Finally, a commercial 12.5 GSPS four-channel TIADC system is utilized to verify the performance of the proposed method. The spurious free dynamic range of the system can be improved by about 20 dB, and the effectiveness of the proposed estimation method is demonstrated.

Published under an exclusive license by AIP Publishing. <https://doi.org/10.1063/5.0103225>

I. INTRODUCTION

Signal sampling and processing applications emerge in many fields, such as radar, 5G communication, and nuclear physics.^{1–3} Analog-to-digital converters (ADCs) are essential components of acquisition systems. To ensure signal fidelity, the sampling rate of acquisition systems is typically three to five times the signal frequency. For some high-speed sampling systems, an ADC with a rate of 10 GHz or higher could be necessary in order to acquire signals at several GHz. However, due to the limitations of the current fabrication process, a single ADC-based acquisition system often cannot meet the requirements of speed. Some studies have focused on addressing this challenge.^{4–7} However, the applicability of these techniques is typically restricted to certain signals or systems. The widely used time-interleaved ADC (TIADC) technique⁸ in acquisition systems is a promising solution for increasing sampling rates. It can be summarized by a bank of sub-ADCs with the same sampling rates but distinct sampling phases, and the samples are obtained by rearranging the output of each sub-ADC.

Ideally, the performance of the TIADC would be comparable to that of a single ADC with a higher sampling rate. Unfortunately, TIADC is a multi-channel parallel sampling architecture, and mismatches between the sub-ADCs, such as gain, offset, and time skew, would seriously degrade the TIADC performance. Therefore, it is necessary to calibrate the mismatch to improve the performance of the acquisition system.

In previous studies, the channel mismatch is often considered as a fixed model, which means that the coefficients of three mismatches are fixed with respect to signals with different frequencies. The mismatches could be estimated by employing a signal with only one harmonic. Upon this assumption, many calibration algorithms have been proposed in the analog or digital domain.^{9–12} Most of them are based on the “estimation-compensation” strategy, in which the mismatch coefficients are calculated first, followed by analog or digital compensation of the estimated values. Generally, analog calibration techniques, such as the sample-and-hold circuits and the controlled delay lines, are used to calibrate the channel mismatch.^{10,13–15} However, the extra device and circuit would

introduce unnecessary noise and increase the power consumption and printed circuit board area. In contrast, digital calibration techniques can effectively overcome the drawbacks of analog calibration. There are several estimation methods, such as sine curve fitting¹¹ and Fourier transform spectrum analysis,^{12,16} which are widely used for gain, offset, and time skew mismatch. Numerous methods have also been introduced specifically for time skew calibration.^{17–24} One of the most widely employed approaches is the correlation-based method, where the time skew is obtained by calculating the correlation function between adjacent channels of TIADCs.^{17–19} Another one is the derivation-based method,^{20–22} which relies on the correlation of the time skew with the derivative of the input signal. Moreover, a variance-based method was developed in Ref. 23. In Ref. 24, a dithering calibration method was described. The channel time skew could be determined by introducing a reference channel and comparing the difference between the sub-ADC and the reference ADC under different dithering signals. For mismatch compensation, it can be implemented by finite impulse response (FIR) filters or fractional delay filters.^{25,26} Interpolation is another type of mismatch error correction technique. For example, a novel FIR filter based on Lagrange polynomial interpolation is reported in Ref. 27. The interpolation coefficients are calculated based on the estimated value of the mismatch error, and then a multichannel Lagrange compensation filter in the form of a FIR filter is performed to compensate for the mismatches. In addition, the Taylor approximation has also been proposed, which requires a derivative filter with fixed coefficients.^{28,29}

A fundamental limitation of the fixed mismatch error model is that the coefficients are unchanged. However, gain and phase will vary with the frequency in the case of wideband signals acquiring, and the fixed mismatch model is a special case at the single frequency point. Numerous techniques are presented to eliminate the variable mismatches.^{30–36} These methods can be mainly divided into two categories: one is based on the perfect reconstruction (PR) method,^{30–32} while the other relies on time-varying filters.^{33–36} The PR strategy is simply a multi-channel compensating filter bank created by computing the inverse matrix of channel frequency responses. In Ref. 33, periodic time-varying filters are applied to correct the mismatches. The fundamental idea underlying the time-varying filter-based method is that the errors can be reconstructed by the time-varying filter and then subtracted from the system output. Calibration is performed entirely in the frequency domain, making it challenging to calculate if the number of channels is large.

In this paper, a strategy that uses a series of sinusoidal signals to estimate the TIADC mismatches is presented. In the previous work,³⁰ a series of sinusoidal signals were used to evaluate the mismatches by sine curve fitting. However, the estimated value of the time skew mismatch may be inaccurate if the signal frequency exceeds the sampling rate of the sub-ADC. The method described in Ref. 31 is similar, except instead of sinusoidal signals, linear frequency modulated (LFM) signals are utilized, and the mismatches can be measured by sampling the LFM signal only once. The advantage of this method is that an LFM signal is substituted for a series of sinusoidal signals, but the samples are divided into multiple small ranges to calculate the mismatch separately, which is similar to sampling the sinusoidal signal multiple times. In comparison with sinusoidal signals, the generation of high-frequency LFM signals is

often expensive. Therefore, a series of sinusoidal signals are adopted to estimate mismatches in this work. In this paper, we propose different estimation methods for the gain and time skew mismatches. Specifically, the contributions of this work are as follows: (1) An autocorrelation-based method to estimate the gain mismatch is presented. The information about the gain mismatch is extracted from the autocorrelation function that is constructed from the sub-ADC output samples. (2) The time skew is estimated using the particle swarm optimization (PSO) algorithm.³⁷ The acquisition system based on TIADC has an equivalent sampling rate that is much higher than the sub-ADC. We tested the proposed approaches with a signal at a frequency that is higher than the Nyquist rate of the sub-ADC, and the result demonstrates that the proposed approaches can achieve high estimation accuracy.

The rest of this paper is organized as follows: Sec. II describes the TIADC acquisition system as well as the signal model. The proposed mismatch estimation approaches are proposed in Sec. III. Section IV reports the simulation and experimental results to investigate the effectiveness of the work. Finally, a conclusion is summarized in Sec. V.

II. THE MODEL OF TIADC SYSTEM

The block diagram of TIADC is shown in Fig. 1. The TIADC system consists of M sub-ADCs with the same resolution and sampling rate, and the input signal is fed into M identical channels. In this structure, ADC_0 samples at a certain sample phase (generally set to 0), and the sampling phases of the other ADCs are delayed relative to this phase, as represented as

$$\varphi_m = 2\pi m/M, \quad m \in [0, M - 1], \quad (1)$$

where φ_m denotes the sampling phase delay of the ADC of the m th channel. The total output is derived from multiplexing the sub-ADC outputs. In this way, the equivalent sampling rate of the TIADC can be increased M times, which means that the equivalent sampling rate of the TIADC is f_s when the sampling rate of a single channel is f_s/M . Ideally, the frequency response of all ADCs is identical, and the

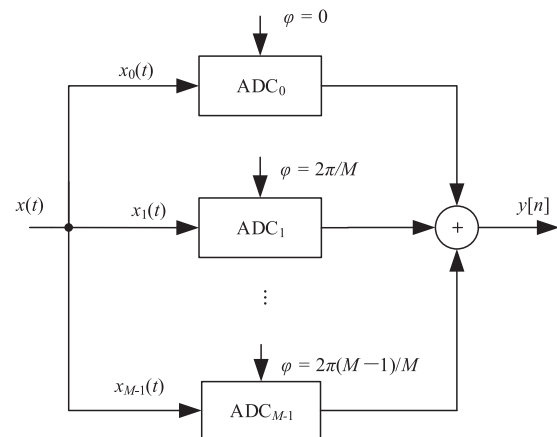


FIG. 1. The block diagram of TIADC.

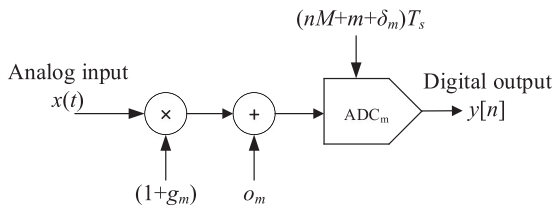


FIG. 2. The diagram of the channel mismatch model.

acquisition system can be seen as a single ADC with a sampling rate of f_s . However, the channel mismatches would seriously degrade the performance of TIADCs. Among the three mismatches, offset mismatch is the easiest to correct since it is independent of the signal frequency.³¹ In this work, we mainly focus on the estimation of the gain and time skew mismatches.

In this paper, a series of sinusoidal signals is adopted to estimate the mismatches of the TIADC. Assuming that the frequency of the k th sinusoidal signal is f_k , the signal can be expressed as

$$x(t) = \sin(2\pi f_k t). \quad (2)$$

Now we consider the channel mismatches, and the output of the m th channel can be expressed as

$$\begin{aligned} y_m[n] &= (1 + g_m) \cdot \sin(2\pi f_k(t_n + \delta_m T_s)) + o_m \\ &= (1 + g_m) \cdot \sin(2\pi f_k(nMT_s + \delta_m T_s)) + o_m, \end{aligned} \quad (3)$$

where g_m , $\delta_m T_s$, and o_m are the gain, time skew, and offset mismatch of the m th channel, respectively. T_s is the sampling period, and M is the number of system channels. The channel mismatch errors model is shown in Fig. 2, where the offset is also taken into account. As the mismatches of the ADC are pooled in the channel frequency response, this model treats all sub-ADCs as ideal. Noting that the gain and time skew vary with signal frequency, a series of sinusoidal signals is employed to estimate the mismatch coefficients at various signal frequencies.

III. PROPOSED METHOD

In this section, the estimation methods of TIADC mismatches are proposed, with a focus on the gain and time skew mismatches.

A. Gain mismatch estimation

In this subsection, an autocorrelation-based approach is proposed to estimate the gain mismatch. The gain mismatch is extracted by calculating the autocorrelation function that is constructed from the sub-ADC output samples. The autocorrelation function only depends on the time interval, and the expression is

$$R_x(t_1, t_2) = R_x(\tau) = E\{x(t + \tau)x(t)\}, \text{ for all } t, \quad (4)$$

where $\tau = t_1 - t_2$. For simplicity, (3) can be rewritten as (the offset mismatch has been ignored)

$$y_m[n] = (1 + g_m) \cdot x(nMT_s + \delta_m T_s). \quad (5)$$

When the time interval is assumed to be zero, the autocorrelation could be represented as

$$\begin{aligned} R_{y_m}(0) &= E\{y_m[n]y_m[n]\} \\ &= E\{(1 + g_m)x(nMT_s + \delta_m T_s)(1 + g_m)x(nMT_s + \delta_m T_s)\} \\ &= (1 + g_m)^2 \cdot R_x(0). \end{aligned} \quad (6)$$

According to (6), the autocorrelation of the m th channel ($0 \leq m \leq M - 1$) could be derived. Specifically, $R_{y_0}(0)$ is

$$R_{y_0}(0) = (1 + g_0)^2 \cdot R_x(0). \quad (7)$$

From (6) and (7), we can get

$$\Gamma_m = \frac{R_{y_m}}{R_{y_0}} = \frac{(1 + g_m)^2}{(1 + g_0)^2}. \quad (8)$$

Generally, channel 0 is always treated as the reference channel, so g_0 is always 0. Therefore, we can obtain the gain mismatches of TIADC channels by (8). The advantage of this approach is that the autocorrelation function is noise-insensitive, and it would be a robust method.

B. Time skew mismatch estimation

In order to estimate time skews of the system precisely, a PSO-based time skew estimation method is proposed, which can extract the time skew mismatch of channels through algorithm iterations.

In the previous work, a method based on Genetic Algorithms (GA)³⁷ has been presented to address the estimation of the mismatches. PSO, which is a similar algorithm to GA, is a population-based stochastic optimization algorithm proposed by Chakravarthi and Bhuma.³⁸ It often requires fewer parameters compared with GA. In this work, a sinusoidal signal is generated based on the potential values of time skew mismatches, followed by the establishment of an error function that indicates the difference between the generated sequence and the actual output of the sub-ADC. More details of the PSO algorithm are shown in Ref. 37. Specifically, the algorithm in this paper can be described as:

- (1) Set up the parameters (parameter initialization). First, randomly generate a population, where the number of particles in the population is also random. Assume that $X_p(\delta_p)$ denotes the p th particle and δ_p represents the value of time skew for the p th particle. Second, randomly initialize the velocity of each particle to ensure that the particles can traverse all possible values of time skews. Meanwhile, the motion boundary of particles should be established according to the range of the time skew. V_p represents the velocity of the p th particle. Furthermore, the number of particles and the iterations of the algorithm should be initialized.
- (2) Calculate the fitness (error) function. Since the input frequency is known in our estimation strategy, we can calculate the theoretical sampling sequence, which can be expressed as

$$x_m[n] = A_m \cos(2\pi f_k t_n) + B_m \sin(2\pi f_k t_n), \quad (9)$$

and

$$\begin{cases} A_m = (1 + g_m) \sin(2\pi f_k \delta_m T_s) \\ B_m = (1 + g_m) \cos(2\pi f_k \delta_m T_s). \end{cases} \quad (10)$$

Note that the gain mismatch g_m is calculated by the autocorrelation function. The coefficient of the time skew δ_m is the only undetermined variable in (9). Therefore, we can substitute the values initialized in the first step into (10), resulting in the following equation:

$$\begin{cases} A_m = (1 + g_m) \sin(2\pi f_k \delta_p T_s) \\ B_m = (1 + g_m) \cos(2\pi f_k \delta_p T_s). \end{cases} \quad (11)$$

Then all the variables in (9) are known. The sequence will be updated as the particles move, and the fitness function can be written as

$$F = \sum_{n=1}^N \{y_m[n] - x_m[n]\}^2. \quad (12)$$

In practice, since channel 0 is the reference channel, the theoretical sampling sequence $x_m[n]$ could be calculated based on the output sequence of channel 0.

- (3) Find the personal best particle [$TB_p(t_b_p)$]. The particles move to different positions as the algorithm iterates. TB_p is the best current position of the p th particle, which has the minimum fitness function value. In the initial stage, $TB_p = X_p$.
- (4) Find the global best particle. Among all the best positions (TB_p) and current particles (X_p), there is a particle with the minimum fitness function value, which is called the global best particle. The index of this particle is denoted as g and can be represented as TB_g .
- (5) Create new particles. The velocity of particles is updated,

$$V_p = \omega V_p + c_1 \cdot rand() \cdot (TB_p - X_p) + c_2 \cdot rand() \cdot (TB_g - X_p), \quad (13)$$

where ω , c_1 and c_2 are constants and $rand()$ generates random values uniformly distributed within $[0, 1]$. Then, we update positions of particles

$$X_p = X_p + V_p. \quad (14)$$

- (6) Update the fitness function. The fitness value is calculated again for the new particles.
- (7) Update the personal best particle and the global best particle. If $F(X_p) < F(TB_p)$, the personal best particle is updated to X_p . Once the personal best particle has been updated, the global best particle should be likewise updated.
- (8) Repeat the steps (5) through (7). After the iteration, when F is minimum, it can be considered that the values of the global best particles TB_g and δ_m are approximately equal.

Now we have obtained the gain and time skew mismatches values for the TIADC system. Note that our analysis is based on a single-frequency signal. The mismatches will change if the frequency is different, and Fig. 3 displays the whole mismatch estimation

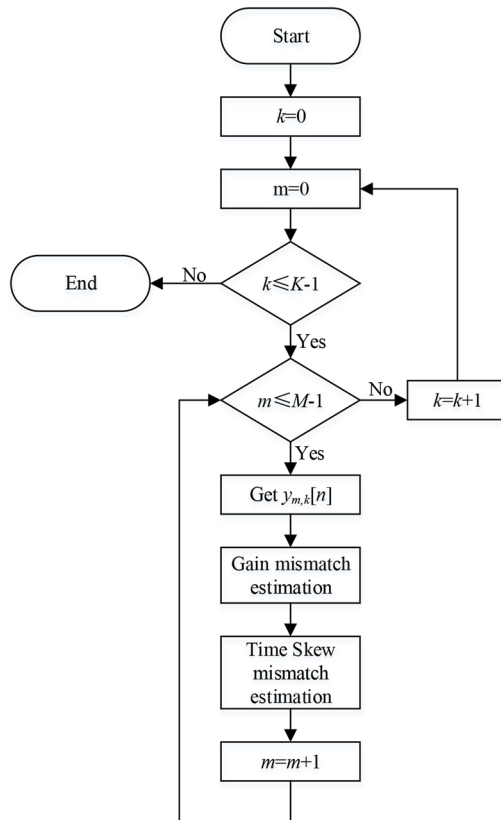


FIG. 3. The flowchart of the mismatch estimation.

method. In Fig. 3, M is the channel number of the TIADC, K represents the number of the sinusoidal signals, and m and k are the channel and sinusoidal signal indices, respectively.

IV. SIMULATION AND EXPERIMENTAL RESULTS

In this section, several simulations and an experiment are performed to investigate the efficiency of the proposed approaches.

A. Simulations

A series of numerical simulations are performed here to explore the feasibility of the proposed approaches. A four-channel TIADC system is applied to acquire signals with different frequencies. The sampling rate of the sub-ADC is 3.125 GSPS, and the total sampling rate is 12.5 GSPS. In order to evaluate the performance of the proposed method at different frequencies, the selected input signal frequencies are 1.0, 1.5, 4.0, and 4.5 GHz, respectively. Note that the signal frequency exceeds the sampling rate of the sub-ADC when the signal frequency is higher than 3.125 GHz, which indicates that the sub-ADC is under-sampling the input signal. The mismatches of different channels are specified in Table I.

In the absence of noise, the performance of the proposed algorithms is initially examined. For the PSO algorithm, we generate

TABLE I. The setting mismatch coefficients.

Sub-ADC	$f_{in} = 1.0 \text{ GHz}$		$f_{in} = 1.5 \text{ GHz}$		$f_{in} = 4.0 \text{ GHz}$		$f_{in} = 4.5 \text{ GHz}$	
	g_m	δ_m	g_m	δ_m	g_m	δ_m	g_m	δ_m
ADC 0	0	0	0	0	0	0	0	0
ADC 1	0.06	0.15	0.18	0.225	-0.1	0.29	-0.08	0.125
ADC 2	0.1	-0.2	0.25	0.14	0.45	0.35	0.25	0.33
ADC 3	-0.15	0.09	0.33	-0.15	-0.32	-0.3	0.1	0.26

TABLE II. The Test Results of the gain mismatch.

Frequency (GHz)	The proposed approach				Sine fitting approach			
	g_0	g_1	g_2	g_3	g_0	g_1	g_2	g_3
1.0	0	0.059	0.10	-0.15	0	0.06	0.10	-0.15
1.5	0	0.179	0.25	0.331	0	0.18	0.25	0.33
4.0	0	-0.10	0.45	-0.32	0	-0.10	0.45	-0.32
4.5	0	-0.08	0.251	0.10	0	-0.08	0.25	0.10

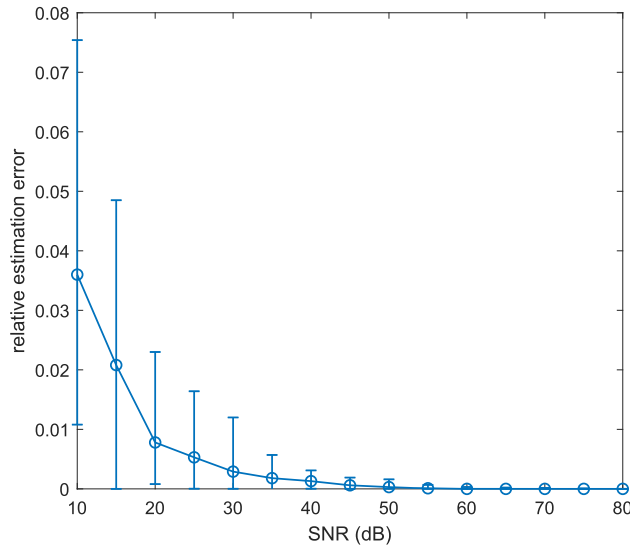
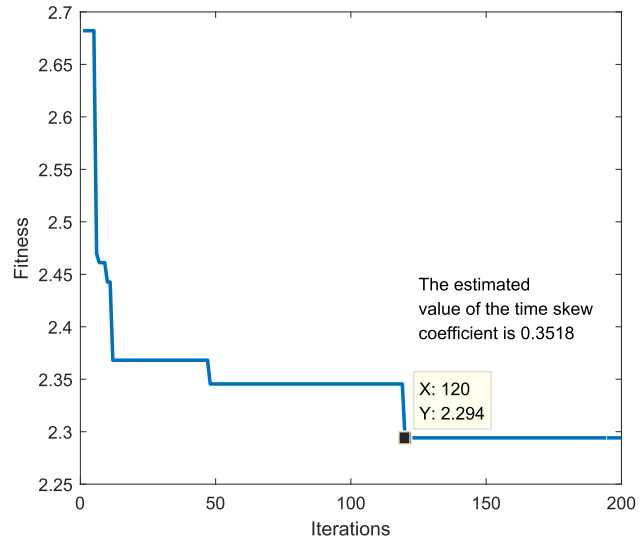
TABLE III. The Test Results of the time skew mismatch.

Frequency (GHz)	The proposed approach				Sine fitting approach			
	δ_0	δ_1	δ_2	δ_3	δ_0	δ_1	δ_2	δ_3
1.0	0	0.15	-0.2	0.09	0	0.15	-0.2	0.09
1.5	0	0.225	0.14	-0.15	0	0.225	0.14	-0.15
4.0	0	0.29	0.35	-0.30	0	0.29	-2.775	-0.3
4.5	0	0.125	0.33	0.26	0	0.125	0.33	-3.6

30 particles randomly. The maximum and the minimum possible values of the time skew coefficient δ_m are set as 1 and -1, respectively. The number of iterations is 200. The estimations of the gain and time skew mismatches are provided in **Tables II** and **III**, respectively, in the columns labeled “the proposed approach.” It shows that the proposed method can estimate the channel mismatches accurately at different frequencies.

In addition, the traditional sine fitting approach^{11,30} is also utilized to estimate the mismatches of the same acquisition system in noise-free conditions. The estimated results are reported in the “sine fitting approach” columns of **Tables II** and **III**, respectively. We note that the sine fitting can estimate the gain mismatch accurately, but sometimes it can produce incorrect results for the time skew mismatch, especially when the signal frequency is higher than the sub-ADC sampling rate. The results show that the proposed method could outperform the sine fitting approach.

In practice, noise will necessarily be present in the acquisition system, which may have an effect on the performance of the estimation method. Therefore, we investigate the robustness of the proposed method to Gaussian white noise. Since the noise does not affect the calculation of the output autocorrelation of each channel,

**FIG. 4.** The average relative estimation errors of the third channel with respect to different SNRs (the input frequency is 4 GHz).**FIG. 5.** The iteration of the PSO algorithm in the third channel (the input frequency is 4 GHz).

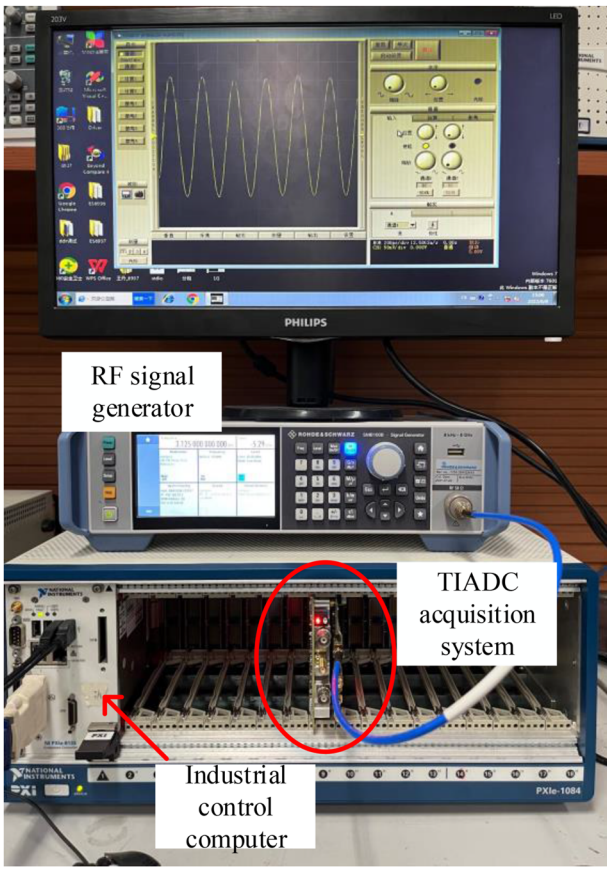


FIG. 6. The diagram of the test hardware platform.

the proposed gain mismatch estimation method has high robustness to noise. We concentrate primarily on the influence of noise on time skew estimation. In order to investigate the effect of noise on the algorithm, we explore the performance of the PSO algorithm under different signal-to-noise ratio (SNR) cases. For simplicity, we

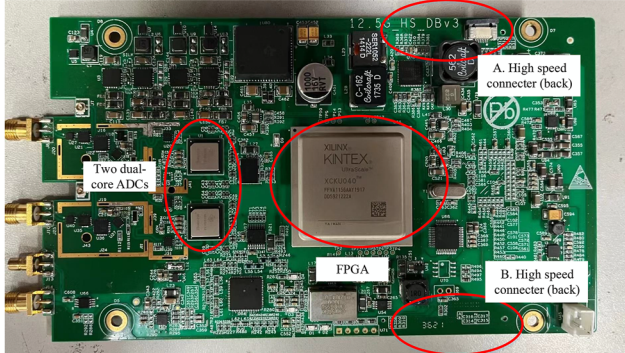
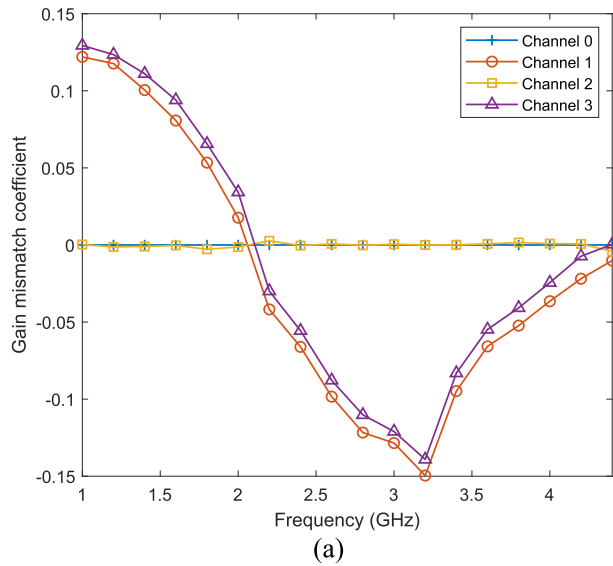


FIG. 7. The prototype of the acquisition system.

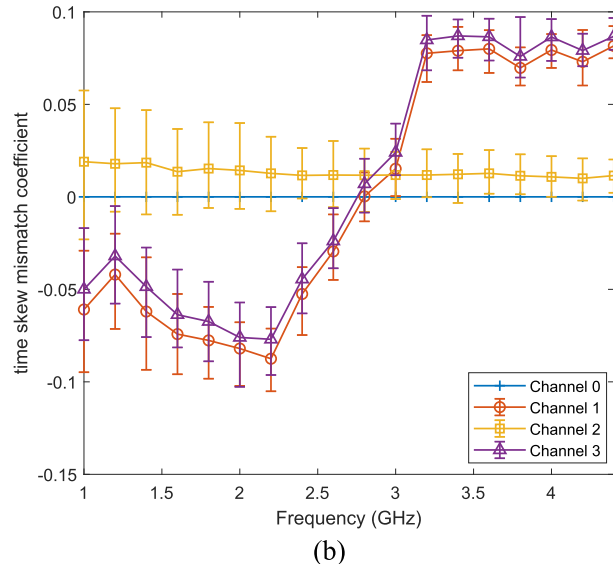
consider one channel (the third channel) with a 4 GHz signal. The coefficient of the time skew mismatch is 0.35, and the relative error is defined as

$$r_e = \frac{|\delta_e - \delta_2|}{\delta_2}, \quad (15)$$

where δ_e is the estimated value of the time skew mismatch and $\delta_2 = 0.35$. The SNR ranges from 10 to 80 dB and 100 trials are performed on each SNR. Figure 4 illustrates the average relative estimation error. It can be seen that the relative error decreases with the increasing SNR, and at the same time, the fluctuation range of the relative error rapidly shrinks. Specifically, Fig. 5 depicts an



(a)



(b)

FIG. 8. Mismatch coefficients estimation: (a) gain mismatch coefficients and (b) time mismatch coefficients.

iterative process of time skew estimation when SNR is 30 dB. It can be noted that the algorithm reaches the global optimal position after 120 iterations. The best value of the fitness function is not zero due to the existence of Gaussian white noise, and the estimated result is 0.3518.

B. Experimental result

The proposed algorithm in this paper is also validated on a hardware platform. The experiment was performed with a four-channel TIADC system, whose total sampling rate is 12.5 GSPS. It is mainly composed of an acquisition module and a processing

module. The acquisition module, shown in Fig. 6, is used to digitize the input signal. The processing module realizes the processing and calibration of the samples, which is completed in Matlab software. A radio frequency (RF) signal generator (SMA 100B from R&S) is used to generate the sinusoidal signals. The signal passes through the conditioning channel, which adjusts the signal to satisfy the input range of ADCs. In order to achieve parallel acquisition, the signal is split up into two paths using a power-splitting network. Then two dual-core ADCs (ADC08DJ3200) are utilized to sample the signals. Each ADC consists of two sub-ADCs with a sampling rate of 3.125 GSPS. After digitizing, the samples are stored and transferred to the computer for processing. A field-programmable gate array (FPGA, XCKU060-2FFVA1156) is used first to store the samples from ADCs, and then the samples are transmitted through the peripheral component interconnect express (PCIE) bus to an industrial control computer. The prototype of the acquisition system is shown in Fig. 7.

In the experiment, the signal with a frequency range of 1.0 to 4.4 GHz with an interval of 200 MHz is used to estimate the gain and time skew mismatch of the channel, and the results are shown in Figs. 8(a) and 8(b), respectively. The channels with even numbers are in the same ADC chip and the channels with odd numbers are in the other chip. It can be seen that frequency mismatches between sub-ADCs in the same chip are smaller than those between chips. Moreover, the mismatches are not fixed over the whole bandwidth, and the fixed mismatch model is no longer applicable in this case.

Based on the estimation results, we investigate the calibration performance of the system. The compensation algorithm of Ref. 30 is adopted in this work, and the signals at 3.7, 3.9, and 4.1 GHz are used to evaluate the calibrated TIADC system. The result is shown in Fig. 9. It can be noted that all the mismatch spurs are reduced after calibration. The improvement of spurious free dynamic range (SFDR) achieved is about 20 dB, which validates the efficiency of the estimation approaches in the acquisition system.

V. CONCLUSIONS

In this paper, we focused on the mismatch estimation of TIADC. The autocorrelation function of the channel output is calculated to measure the gain mismatch. For the time skew mismatch, we proposed a PSO-based algorithm. The gain mismatch is not incorporated in the PSO algorithm because when we introduce the gain mismatch in the current model, the accuracy of the training results decreases significantly, and the convergence rate is also slower. Some simulations and experiments are performed to evaluate the proposed approaches. The proposed algorithms were investigated at different frequency points, and the results have demonstrated the applicability and feasibility of the method. It provides an idea to estimate mismatches by using intelligent algorithms. However, the complexity of the estimation algorithm will increase with the channel number of the system, and improving the convergence rate of the algorithm is one of the future tasks in this field.

ACKNOWLEDGMENTS

This work was supported, in part, by the National Natural Science Foundation of China under Grant No. 61671114 and the Fundamental Research Funds for the Central Universities under Grant No. ZYGX2020ZB001.

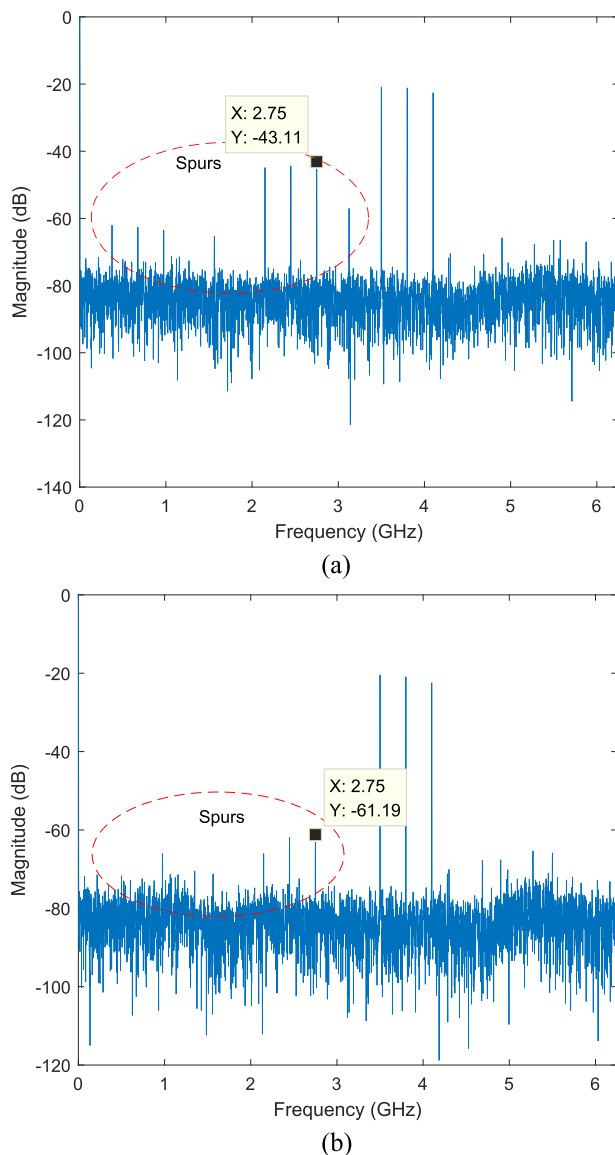


FIG. 9. Sinusoidal signal calibration performance: (a) before calibration and (b) after calibration.

AUTHOR DECLARATIONS**Conflict of Interest**

The authors have no conflicts to disclose.

Author Contributions

Yanze Zheng: Conceptualization (equal); Formal analysis (lead); Methodology (lead); Software (equal); Validation (equal); Writing – original draft (lead). **Naixin Zhou:** Data curation (equal); Software (equal); Writing – review & editing (equal). **Yijiu Zhao:** Project administration (lead); Supervision (equal). **Sicheng Sun:** Investigation (equal); Resources (equal); Software (equal).

DATA AVAILABILITY

Data sharing is not applicable to this article as no new data were created or analyzed in this study.

REFERENCES

- ¹F. Maloberti, *IEEE Circuits Syst. Mag.* **1**(1), 26–36 (2001).
- ²M. G. Sánchez, M. P. Táboas, and E. L. Cid, *Measurement* **95**, 223–229 (2017).
- ³E. C. Pollacco, G. F. Grinyer *et al.*, *Nucl. Instrum. Methods Phys. Res., Sect. A* **887**, 81–93 (2018).
- ⁴S. Jiang, N. Fu, Z. Wei *et al.*, *IEEE Trans. Instrum. Meas.* **71**, 1–15 (2022).
- ⁵Y. Zhao, Y. H. Hu, and J. Liu, *IEEE Trans. Instrum. Meas.* **66**(7), 1789–1797 (2017).
- ⁶Y. Zhao, H. Wang, Y. Zheng *et al.*, *Measurement* **166**, 108175–108182 (2020).
- ⁷N. Fu, Z. Wei, L. Qiao, and Z. Yan, *IEEE Trans. Instrum. Meas.* **69**(9), 6853–6869 (2020).
- ⁸W. C. Black and D. A. Hodges, *IEEE J. Solid-State Circuits* **15**(6), 1022–1029 (1980).
- ⁹S. Huang and B. C. Levy, *IEEE Trans. Circuits Syst. I* **53**(6), 1278–1288 (2006).
- ¹⁰H. Wei, P. Zhang, B. D. Sahoo, and B. Razavi, *IEEE J. Solid-State Circuits* **49**(8), 1751–1761 (2014).
- ¹¹Y. Park, J. Kim, and C. Kim, *IEEE Trans. Circuits Syst. I* **63**(11), 1889–1897 (2016).
- ¹²L. Guo, S. Tian, and Z. Wang, *Metrol. Meas. Syst.* **21**(3), 535–544 (2014).
- ¹³A. Leuciuc, in *2017 IEEE International Symposium Circuits and Systems (ISCAS)* (IEEE, 2017), pp. 1–4.
- ¹⁴J. Song, K. Ragab, X. Tang, and N. Sun, *IEEE J. Solid-State Circuit* **52**(10), 2563–2575 (2017).
- ¹⁵M. El-Chammas and B. Murmann, *IEEE J. Solid-State Circuit* **46**(4), 838–847 (2011).
- ¹⁶K. Yang, Z. Pan, P. Ye *et al.*, *Rev. Sci. Instrum.* **92**, 054709 (2021).
- ¹⁷X. Wang, F. Li, W. Jia, and Z. Wang, *IEEE Trans. Circuits Syst. II* **66**(3), 322–326 (2019).
- ¹⁸A. Salib, M. F. Flanagan, and B. Cardiff, *IEEE Trans. Circuits Syst. I* **66**(10), 3747–3760 (2019).
- ¹⁹H. Le Duc, D. M. Nguyen, C. Jabbour *et al.*, *IEEE Trans. Circuits Syst. I* **64**(6), 1515–1528 (2017).
- ²⁰D. Stepanovic and B. Nikolic, *IEEE J. Solid-State Circuits* **48**(4), 971–982 (2013).
- ²¹H.-W. Kang, H.-K. Hong, W. Kim, and S.-T. Ryu, *IEEE J. Solid-State Circuits* **53**(9), 2584–2594 (2018).
- ²²Y. Zhou, B. Xu, and Y. Chiu, *IEEE J. Solid-State Circuits* **54**(8), 2207–2218 (2019).
- ²³J. Song, K. Ragab, X. Tang, and N. Sun, *IEEE Trans. Circuits Syst. I* **66**(8), 2876–2887 (2019).
- ²⁴B. Xu, Y. Zhou, and Y. Chiu, *IEEE J. Solid-State Circuits* **52**(4), 1091–1100 (2017).
- ²⁵J. Wei, M. Liu, Z. Zhu, and Y. Yang, in *2020 IEEE 15th International Conference on Solid-State and Integrated Circuit Technology (ICSICT)* (IEEE, 2020), pp. 1–3.
- ²⁶L. Qiu, K. Tang, Y. Zheng, L. Siek, Y. Zhu, and S.-P. U, *IEEE Trans. Very Large Scale Integr. Syst.* **26**(3), 572–583 (2018).
- ²⁷Y. Zou, S. Zhang, Y. Lim, and X. Chen, *IEEE Trans. Instrum. Meas.* **60**(4), 1123–1131 (2011).
- ²⁸H. Chen, L. Wang, R. Xiao, Y. Yin, H. Deng, and X. Meng, in *2021 IEEE International Conference on Integrated Circuits, Technologies and Applications (ICTA)* (IEEE, 2021), pp. 41–42.
- ²⁹M. Yin and Z. Ye, *IEEE Trans. Circuits Syst. II* **67**(1), 162–166 (2020).
- ³⁰J. Li, J. Pan, and Y. Zhang, *Electronics* **8**, 56 (2019).
- ³¹X. Peng, Y. Zhang, W. Wang, and S. Yang, *IEEE Trans. Circuits Syst. I* **68**(9), 3621–3630 (2021).
- ³²F. Rosato, P. Monsurrò, and A. Trifiletti, *2017 European Conference on Circuit Theory and Design (ECCTD)* (IEEE, 2017), pp. 1–4.
- ³³C. Vogel and S. Mendel, *IEEE Trans. Circuits Syst. I* **56**(11), 2463–2475 (2009).
- ³⁴Z. Pan, P. Ye *et al.*, *Rev. Sci. Instrum.* **92**, 064711 (2021).
- ³⁵H. Johansson, *IEEE J. Sel. Top. Signal Process.* **3**(3), 384–396 (2009).
- ³⁶W. Wei *et al.*, *IEICE Electron. Express* **17**(22), 1–6 (2020).
- ³⁷J. Kennedy and R. C. Eberhart, in *Proceedings of ICNN'95—International Conference on Neural Networks* (IEEE, 1995), pp. 1942–1948.
- ³⁸M. V. Chakravarthi and C. M. Bhuma, in *2017 14th IEEE India Council International Conference (INDICON)* (IEEE, 2017), pp. 1–6.